Thermal Performance of a Graphite Foam Material with Water Flow for Cooling Power Electronics

by

Richard W. Garman, Ryan J. Elwell
Anteon Corporation, Machinery Systems Department
Annapolis, MD 21402

Abstract

A critical factor affecting the operating life and limitations of a power semiconductor is the temperature of its junction. Numerous heat sinks and heat transfer devices have been designed and developed to remove heat from power semiconductors. One potential thermal management solution evaluated under this program is high thermal conductivity graphite foam. This material has a thermal conductivity roughly equivalent to aluminum 6061, but with one-fifth the weight. The thermal performance for three configurations of the foam was tested using cooling water and the results compared.

Introduction

A study is ongoing to quantify and determine alternative methods to maintain thermal equilibrium for an advance linear motor (ALM) for use in an electric aircraft recovery system (EARS). The study is being conducted by the Machinery Systems Department of Anteon Corporation and funded by the Office of Naval Research (ONR), through the Naval Air Warfare Center, Aircraft Division (NAWCAD) at Lakehurst, NJ. One focus of the thermal management effort is on the direct ALM, mainly the stators and armature. A second focus is the power conversion and control subsystems, which will be made up of power electronics requiring enhanced thermal management.

The NAWCAD sponsor brought an innovative graphite foam material[a], which was developed at the Oak Ridge National Laboratory (ORNL), to the attention of Anteon. After discussions with personnel from the ORNL, several different configurations of the graphite foam material were provided to Anteon for testing. The samples were tested in the power electronic thermal management test facility developed by Anteon Corporation, under the power electronics building blocks (PEBB) program. In these tests, water is used as the cooling fluid.

Background

The thermal performance of the graphite foam material was quantified for consideration in cooling power electronic devices in the EARS ALM power conversion and control subsystems. The heat generated in these power semiconductor devices is due to large pulse current and must be removed to control the junction temperature. Through effective removal of heat from the junction, the power rating of the devices can be maximized and the size minimized. Conversely, if adequate cooling is not provided, the devices will fail prematurely. Heat is typically conducted in these devices through the silicon to copper conductors, then through solder and one or more metalization and thermal expansion layers to a ceramic baseplate connected to a heat sink.

---

[a] Licensed for manufacture to Poco Graphite, Inc., 1601 South State Street, Decatur, Texas 76234.

This section will provide a brief description of the graphite foam, the test facilities, the experimental procedures and the three different configurations tested. The tests were performed in the facility originally developed to characterize heat sink thermal performance under the Navy's PEBB program. Thermal impedance was selected as the primary measure of the thermal performance of each heat sink sample because it provides a basic measure, independent of the heat source. A thermal resistance value was also estimated and presented as a measure consistent with industry standards.

Graphite Foam

The development of new, lightweight foams has led to innovative, light-weight, high strength, carbon based materials. These materials are typically pitch derived using traditional blowing and oxidative stabilization steps to manufacture and result in low thermal conductivities. These carbon-based materials can even act as thermal insulators. The Carbon and Insulation Materials Technology Group at the ORNL recently developed a less time consuming process for fabricating a pitch-based graphite foam. The new foams exhibit a high thermal conductivity, nearly equivalent to aluminum 6061, but with one-fifth the weight. It is anticipated that this new graphite foam material will be less expensive and easier to manufacture.[1]

Test data presented by ORNL shows that the thermal conductivity of these graphite materials varies linearly with density. For a range of densities between 270 to 570 kg/m^3, the thermal conductivities vary from 50 to 150 W/m-K. Several thermal management materials have a higher thermal conductivity, such as copper (400 W/m-K), but they are also much heavier (8900 kg/m^3). When a comparison of the specific thermal conductivity (defined as the thermal conductivity divided by the specific gravity) is made, the graphite foam has exhibited specific thermal conductivities over 300 W/m-K, which is roughly five times higher than aluminum (64 W/m-K) and six times higher than copper (45 W/m-K).[1]

The coefficient of thermal expansion (CTE) of the foam may also offer a benefit for power electronics applications. The CTE of the ORNL foam[2] is in the range of 2 – 3 ppm/°C, versus 17 ppm/°C for copper[3] and 23 ppm/°C for aluminum[3]. The graphite foam CTE is much closer matched to the silicon chip (2.6 ppm/°C)[3] and the CTE of typical baseplate ceramics, such as Aluminum Nitride (CTE of 3.3 ppm/°C)[3]. This may help reduce thermal stresses attributed to high mismatches in CTE values and thereby, improving reliability.

The foam-based structure is extremely versatile, easily machined, and can be made into various sized samples in virtually any configuration. The foam is a porous material and can be manufactured with varying degrees of porosity. The foams have shown potential benefits through successful demonstrations of densification with aluminum, carbon epoxy, and thermoplastic resins. The graphite foam applications have also been demonstrated as reinforcement in composite structures where high thermal conductivity is required.[1]

Potential applications of the graphite foam are still being explored, but thermal management has been the focus since its development. A majority of published work by ORNL regarding this material is for forced-air thermal management systems. One test compared a standard aluminum finned heat sink used in a Pentium 133 microprocessor to a similar geometry device machined from a graphite foam sample. The graphite foam heat sink out performed the aluminum heat sink, which had a mass 5.5 times larger. In follow-on testing, the fins were machined off the graphite foam heat sink and a similar experiment was conducted. The graphite foam showed slightly less thermal performance, but its mass was eleven times smaller. For an additional test, an identical finned heat sink was machined from the graphite foam material and installed in an operational Pentium 133 computer. This computer has operated with the original cooling fan, without problems, for over a year.[1]

Several items make this material an attractive candidate for use in cooling Navy power electronic devices associated with the ALM subsystems. First, the high heat conductivity may allow for enhanced heat transfer to occur. Second, most Navy applications are very volume and weight sensitive. This

material may help to reduce the overall package size. Finally, there are benefits from low material costs and ease of manufacturing.

Test Facility

A schematic of the experimental test facility is shown in Figure 1[4]. There are three main parts to this test facility: the water circulation loop, the heat generation components, and the instrumentation. Water is circulated at a controlled temperature from the chiller bath via a circulating pump with the flow rate controlled by a bypass flow control valve. Heat is generated by a thick film resistor (TFR) connected to a 15 kW power supply. The instrumentation consists of two thermistor probes, two pressure gauges, two digital multimeters, a flow meter, and an infrared thermal imaging camera to record the temperature profile at the top surface of the TFR.

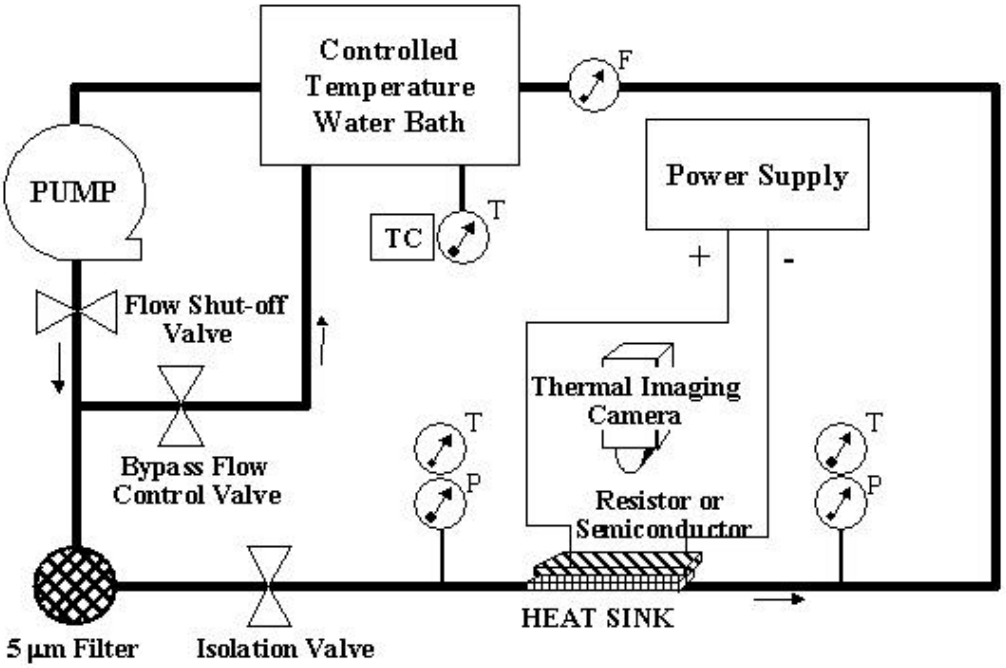

Figure 1. Thermal Management Laboratory Schematic

Experimental Procedure

The experimental procedure focused on the cooling performance of the heat sink, represented by the thermal impedance, and from a systems perspective through the pressure drop. The thermal impedance, shown in equation (1)[5], is defined as the temperature differential required for a unit heat flux,

$$q_{sink}(x,y) = \frac{T(x,y) - T_F}{(q/A)_{sink}(x,y)}, \quad \textbf{(1)}$$

where $\theta_{sink}(x,y)$ is the heat sink thermal impedance, $T(x,y)$ is the temperature distribution over the heat sink interface with the heat source, T_F is the bulk cooling fluid temperature, and $(q/A)_{sink}(x,y)$ is the heat flux through the interface.[5]

From equation (1), it can be noted that the thermal impedance and heat flux are spatially varying quantities defined over the interface. In contrast, the more commonly used thermal resistance is a single point value that is determined in a manner that allows the use of an electrical analogy in solving thermal calculations. The thermal resistance value is typically calculated for a specific heat sink and device

combination. An estimated value of the thermal resistance is presented in this paper. The thermal impedance value was divided by the area of the heat source to calculate the thermal resistance. It is also important to note that the thermal impedance value is merely the inverse of the overall heat transfer coefficient.[5]

The experimental measurements of the thermal impedance involve measuring the fluid inlet and outlet temperatures, the temperature distribution over the interface between the heat sink and the thermal load, and the heat flux at the same interface. Measurements of the fluid temperature are straightforward. The remaining quantities were determined by temperature measurements across the TFR using the infrared camera and the power (voltage and current) across the TFR. The temperature at the bottom surface of the TFR and heat sink junction is easily calculated using the temperature dependent thermal conductivity of the TFR material. The heat flux at the TFR interface with the heat sink is determined by subtracting the heat flux due to radiation and natural convection, calibrated prior to testing, from the heat generated by the resistor.[5]

Graphite Foam Configurations

Three configurations of the graphite foam were tested. The samples were provided by ORNL to characterize the performance of the graphite foam with water-cooling and were in no way optimized for thermal performance. The first sample, Foam #17, is made of high-density graphite foam with vertical blind holes drilled perpendicular to the flow. The second sample, Foam #18, is solid, low-density graphite foam. The final sample, Foam #20, is high-density graphite foam with horizontal blind holes drilled parallel to the flow. A fourth graphite foam sample, Foam #19, was provided by ORNL for testing, but the TFR cracked during the test set up and was unusable for testing.

All three foam samples were tested with flow rates of 0.5, 1.0, 2.0, 3.0, and 3.5 gpm of water. Data was taken for at least three power levels for each sample at each flow rate. A power of 200 W was the minimum level set and increased in 200 W increments until a mean temperature of approximately 100 °C was reached. Previous testing revealed that a temperature value of 100 °C provided a safe maximum operating limit for the TFR. Cavity heat sinks tested above this level under the PEBB program caused the TFR to crack due to stresses believed to be caused by localized boiling under the TFR surface. This is a conservative value for the graphite foam tests due to the structural stability and mass of the foam. In separate high temperature tests, each sample was tested to 125 °C.

Test Results

The plots contained in Figure 2 to Figure 4 compare the thermal impedance performance versus cooling water flow rate for the three graphite foam configurations tested. Figure 2 is a plot of the average thermal impedance versus flow rate and Figure 3 is a plot of the thermal impedance standard deviation versus flow rate. Figure 4 is a plot of the average thermal impedance plus one standard deviation versus flow rate, i.e. the sum of the values plotted in Figure 2 and Figure 3.

Figure 2 clearly shows that the high-density graphite foams out performed the low-density foam. This was expected since the higher density foams have a corresponding higher thermal conductivity, which translates to faster heat transfer from the heat source. Foam #20, with the horizontal blind holes, out performed Foam #17, with the vertical blind holes. The thermal performance of Foam # 20 is roughly 1.5 times higher than Foam #18 at the high flow rates and almost twice as high at the low flow rates. Foam #20 thermal impedance varies from 1.5 to 1.3 times lower than Foam #17 as the flow is increased.

The plot of the thermal impedance standard deviation versus flow rate, shown in Figure 3, reveals similar results to Figure 2. Foam #20 also had the lowest standard deviation. However, the curve trends differ from the plot in Figure 2. Each standard deviation curve slopes downward, reaches a minimum, and then creeps slightly upward. The minimum value is reached at lower flow rates for the configurations with lower thermal impedance (better thermal performance). Figure 3 also shows that Foam #20 provided more uniform cooling than the other two samples. This is in agreement with the thermal impedance data.

Since Foam #20 provides better cooling, the isometric temperature contours are smaller, hence, lower thermal impedance standard deviations.

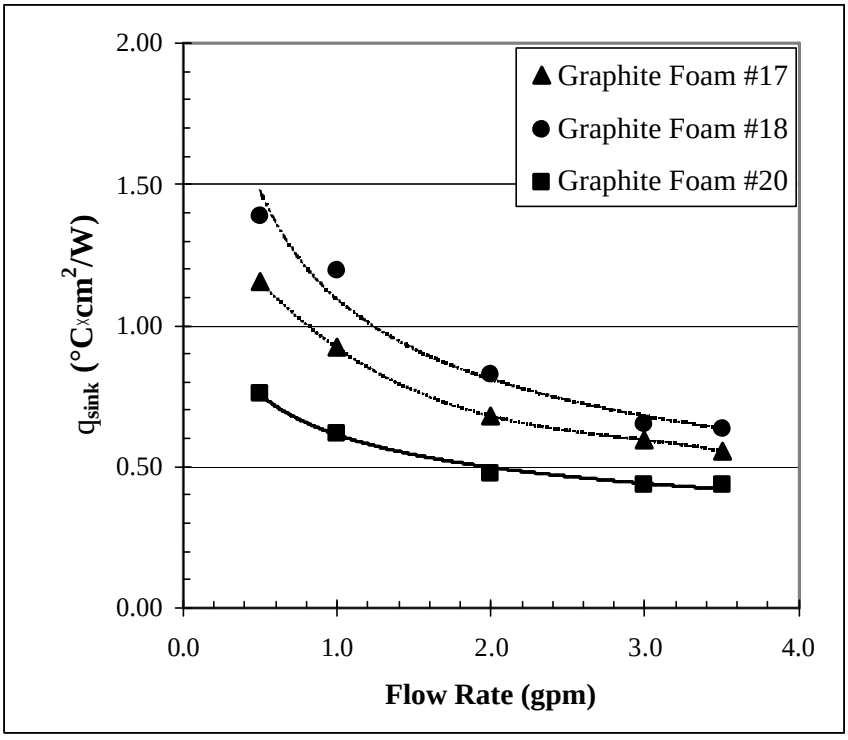

Figure 2. Average Thermal Impedance vs. Cooling Water Flow Rate

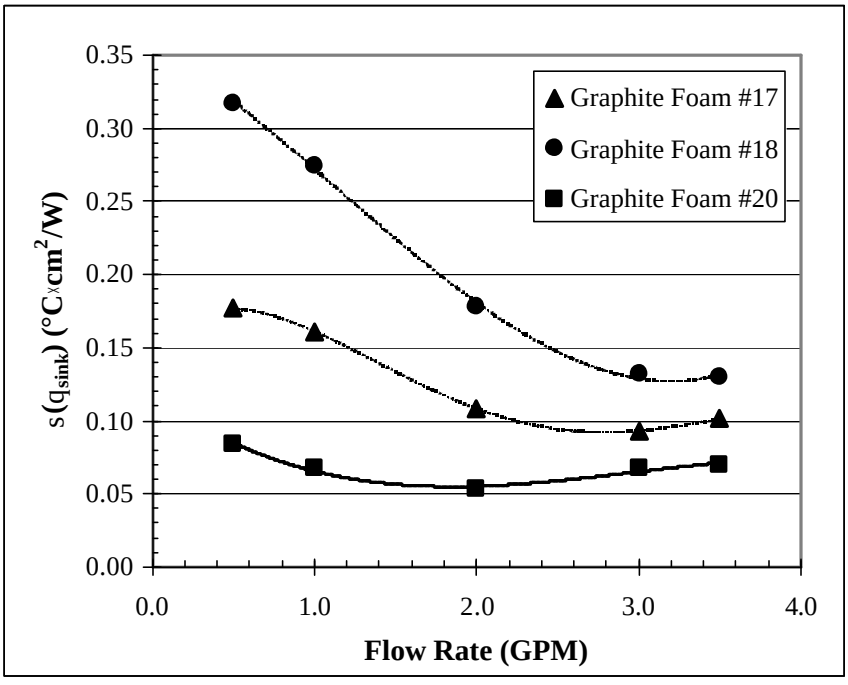

Figure 3. Thermal Impedance Standard Deviation vs. Cooling Water Flow Rate

Figure 4 is a plot of the thermal impedance plus one standard deviation versus flow rate. The purpose of this figure is to compare each configuration based on the less effectively cooled areas. For a normal Gauss distribution of samples (e.g., the familiar bell curve), the range from the average minus one standard deviation to the average plus one standard deviation contains 68% of the samples. If the assumption is made here that the values of the thermal impedance at each pixel from the infrared image form a normal distribution, then 84% of the TFR would have a thermal impedance less than the average plus one standard deviation. Therefore, by comparing configurations based on the average plus one standard deviation, a more useful uniformity conclusion can be drawn. That is, the majority of the heat sink area can be expected to have thermal impedance values lower than the value plotted in Figure 4. This confirms the results of the previous two plots.

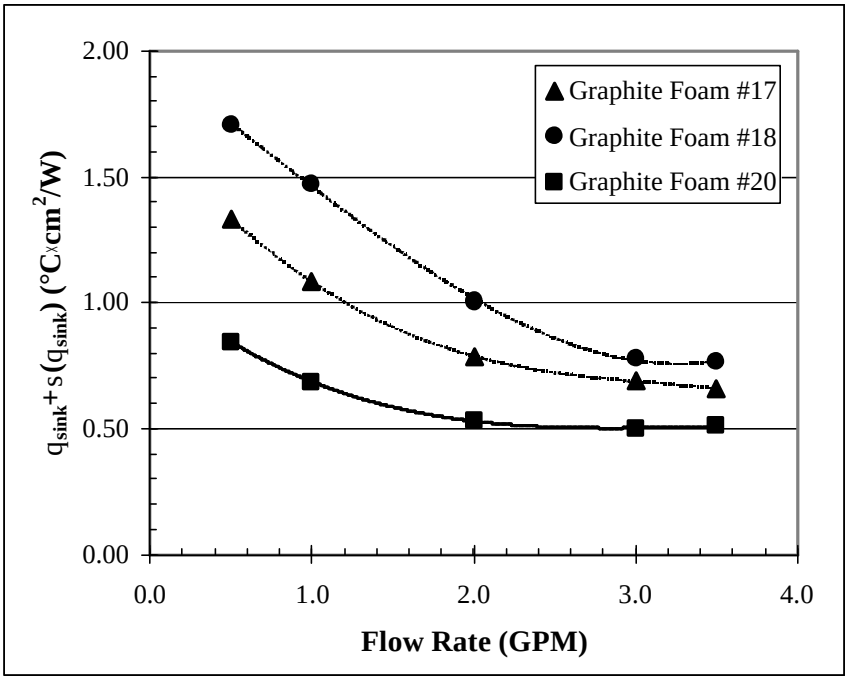

Figure 4. Average Thermal Impedance Plus One S.D. vs. Cooling Water Flow Rate

Figure 5 is a plot comparing the pressure drop versus flow rate. By comparing this plot to Figure 2, there is a general inverse trend between the thermal impedance of the heat sink and the pressure drop of the cooling water through them. A heat sink providing lower thermal impedance tends to have added cost in the form of a larger pressure drop. This is expected because good heat transfer from a surface to a fluid comes from having a thin boundary layer with a high thermal gradient within the boundary layer. Good fluid mixing and a turbulent boundary layer produce these characteristics, and both tend to increase the resistance to flow. The good news in Figure 5 is that Foam #20 remains relatively low, especially when compared to the other high-density foam, which has higher thermal impedance. It is interesting to note that vertical blind holes reduced the pressure drop by 50% over a solid (porous) foam in testing performed by ORNL using air as the working fluid, while maintaining a higher heat transfer.[6]

Figure 6 is a means to compare the foam configurations in terms of the average thermal impedance plus one standard deviation versus fluid or pumping power. Figure 7 is the same plot on a logarithmic scale. Stating which configuration is best in these plots depends upon important design criteria. If a value of the thermal impedance is sought at the lowest pumping power cost, then the left-most curve for that thermal impedance would be best. If the lowest thermal impedance for an available pumping power is sought, then the lowest curve for that pumping power would be best. Foam #20 meets

both of these criteria to provide the best cooling performance for a given flow rate or pumping power. Foam #17 may be selected to minimize system cost.

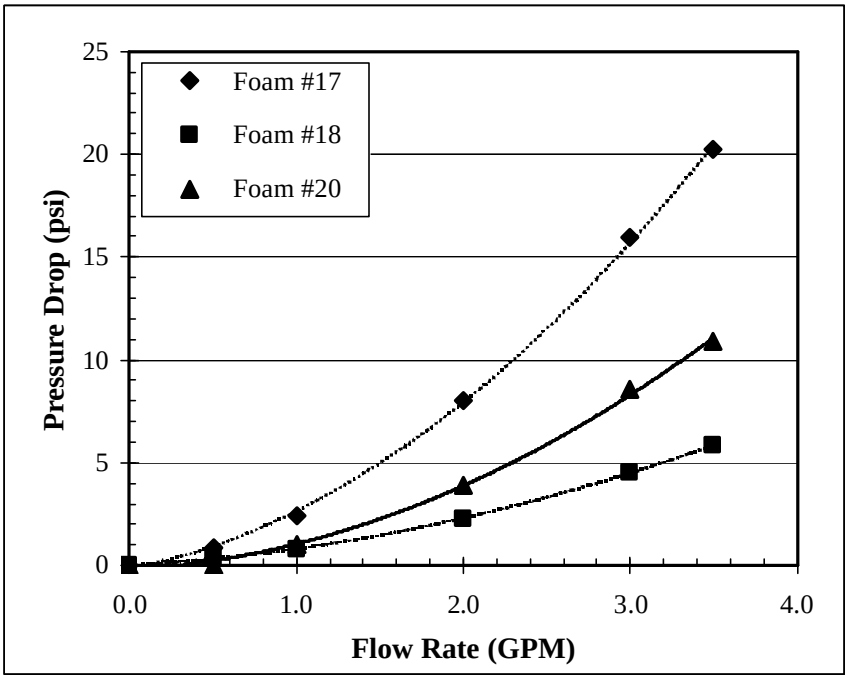

Figure 5. Pressure Drop vs. Flow Rate

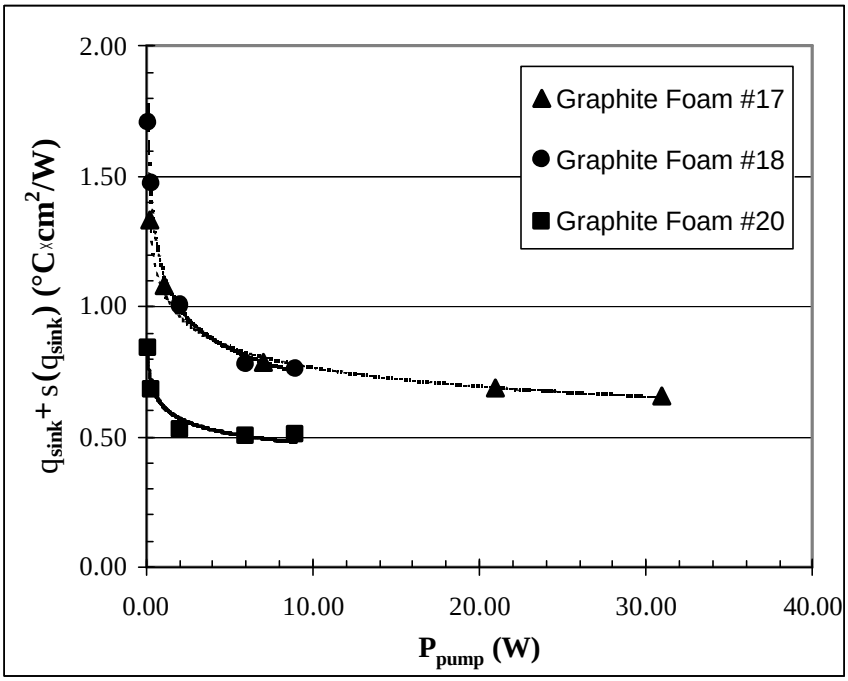

Figure 6. Average Thermal Impedance Plus One S.D. vs. Cooling Water Pumping Power

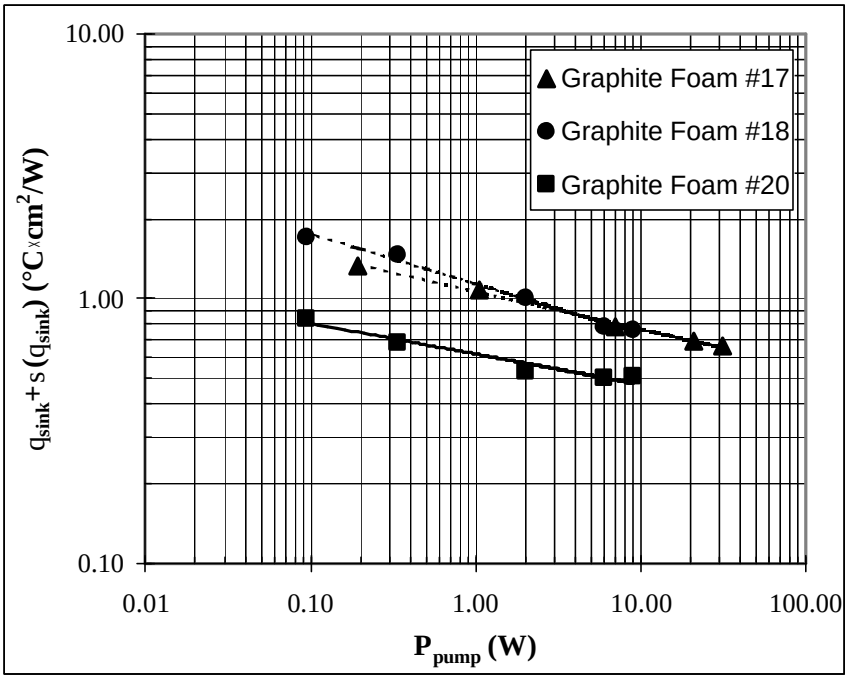

Figure 7. Average Thermal Impedance Plus One S.D. vs. Cooling Water Pumping Power (log plot)

Table 1 contains a list of the estimated thermal resistance of each foam at the test flow rates. These values are calculated from the thermal impedance measurements and therefore follow the same trends as the thermal impedance.

Table 1. Estimated Graphite Foam Thermal Resistance

Flow Rate (gpm)	$R_{Foam\ \#17}$ (°C/W)	$R_{Foam\ \#18}$ (°C/W)	$R_{Foam\ \#20}$ (°C/W)
0.5	0.0691	0.0832	0.0456
1.0	0.0552	0.0718	0.0370
2.0	0.0407	0.0495	0.0286
3.0	0.0356	0.0389	0.0260
3.5	0.0333	0.0379	0.0263

ORNL has published several studies involving air-cooled graphite foam heat sinks. Table 2 provides a comparison between air-cooled data published in reference 6 and the water-cooled data presented in this paper. This table shows that water-cooling has over a tenfold enhancement in heat transfer at much lower fluid volumetric flow rates. As noted, the ORNL test data is for a high-density foam, similar in configuration to Foam #17, with vertical blind holes. The diameter and pattern of the vertical blind holes were similar, however, the foam tested by ORNL was approximately twice the size of the foam configurations tested with water-cooling.

Table 2. Overall Heat Transfer Coefficient Comparison Between Water Cooling and Air Cooling

Water Flow Rate (LPM)	$h_{Foam\ \#17}$ (W/m^2-°C)	$h_{Foam\ \#18}$ (W/m^2-°C)	$h_{Foam\ \#20}$ (W/m^2-°C)	**Air Flow Rate (LPM)**	**h_{Foam}[b] (W/m^2-°C)**
1.89	8,662	7,195	13,140	145	1,185
3.78	10,850	8,343	16,200	230	1,500
7.57	14,710	12,100	20,920	285	1,600
11.4	16,810	15,380	23,050	340	1,730
13.2	17,960	15,790	22,800	400	1,910

Conclusions

The test results obtained for the three graphite foam samples are promising. The graphite foams can be used to efficiently remove heat from power electronic devices. The high-density foam with horizontal blind holes had the best thermal performance. Its pressure drop was also considerably lower than the other high-density foam (Foam #17) configuration tested. A maximum power density measured in this work approached 70 W/cm^2 and was dissipated with Foam#20 at a mean TFR surface temperature of 96 °C.

The lightweight, high conductivity graphite foam presents an innovative solution to thermal management of power electronics systems. This effort studied only a few configurations. Other configurations, such as extruding fins, channel flow, or post heat sink designs should be considered. The ease of machining this material will allow for inexpensive testing of other configurations. One drawback of this material is that it is new and relatively untested in commercial applications. Durability and reliability in a water flow thermal management system is unknown.

The primary thermal management application of this material is in air-cooled systems. Testing the graphite foam for a water-cooled electronic application is novel. The data previously reviewed for air cooling show air-cooled heat sinks made from the graphite foam have been able to dissipate a maximum power around 25 W/cm^2. However, this power density was achieved at a heater temperature of approximately 150 °C. An extrapolation of the Foam #20 test data at a water flow rate of 3.5 gpm, for an average TFR surface temperature to 150 °C, shows that a power density around 120 W/cm^2 can be achieved.

This paper reports on an initial look at this novel material using water-cooling. These results show that the graphite foam is a promising thermal management material. However, additional testing and development of the material is required prior to utilization in any power electronics systems with water flow cooling.

Acknowledgments

The authors are grateful to the Office of Naval Research and the Naval Air Warfare Center, Aircraft Division, Lakehurst, NJ for their support. The authors are also appreciative of the efforts of Dr. James Klett and his staff at the Oak Ridge National Laboratory, Metals and Ceramics Division, for supplying and preparing the graphite foam samples for testing.

[b] This test foam is similar to Foam #17, a high-density foam with vertical blind holes.

References

1. James Klett and Bret Conway, “Thermal Management Solutions Utilizing High Thermal Conductivity Graphite Foams.”
2. James Klett, “High Thermal Conductivity Graphite Foams, One Pager (Physical Properties, Mechanical Properties, and Thermal Properties),” Oak Ridge National Laboratory, Carbon and Insulation Materials Technology Group.
3. Rao Tummala, Eugene Rymaszewski, & Alan Klopfenstein, Microelectronics Packaging Handbook, Book I: Technology Drivers, Van Nostrand Reinhold, 1997.
4. Dr. Peter N. Harrison and Richard W. Garman, “PEBB Thermal Management Baseline Study Test Plan,” A&T Engineering Technologies, VECTOR Research Division, July 8, 1998.
5. Dr. Peter N. Harrison and Richard W. Garman, “PEBB Thermal Management Interim Report,” A&T Engineering Technologies, VECTOR Research Division, May 28, 1999.
6. Dr. James Klett, “High Thermal Conductivity, Mesophase Pitch-Derived Carbon Foams,” Presentation by the Metals and Ceramics Division, Oak Ridge National Laboratory, 2000.